J Mol Model (2013) 19:3581–3589
DOI 10.1007/s00894-013-1887-8

ORIGINAL PAPER

Structure guided inhibitor designing of CDK2 and discovery of potential leads against cancer

Arun Kumar V.A · Keshav Mohan · Syed Riyaz

Received: 20 March 2013 / Accepted: 6 May 2013 / Published online: 1 June 2013

Abstract On the basis of stereo specific information obtained from crystal structures of CDK2, indole and chromene analogues were designed by suitably substituting the pharmacophores on their moiety and docked with target protein for calculating binding affinities. The binding affinities are represented in glide score. (5*E*)-5-[(1-methyl-1*H*-indol-3-yl)methylidene]-2,4,6-trioxotetrahydro-2*H*-pyrimidin-1-ide (I_1), (5*E*)-5-(1*H*-indol-3-ylmethylidene)-2,4,6-trioxotetrahydro-2*H*-pyrimidin-1-ide (I_2) and 2-amino-4-(4-methyl phenyl)-5-oxo-5,6,7,8-tetrahydro-4*H*-chromene-3-carbonitrile (C_9) were selected for synthesis and biological testing based on vital interactions. (5*E*)-5-(1*H*-indol-3-ylmethylidene)-2,4,6-trioxotetrahydro-2*H*-pyrimidin-1-ide (I_2) and 2-amino-4-(4-methyl phenyl)-5-oxo-5,6,7,8-tetrahydro-4*H*-chromene-3-carbonitrile (C_9) were proved to be active against MCF-7 and HeLa cell lines.

Keywords CDK · HeLa · MCF-7 · Pharmacophores

Introduction

Cancer begins when cells in a part of the body start to grow out of control. There are many kinds of cancer and the common treatment protocol for cancer involved surgery, radiation and chemotherapy. Cancer is the second leading cause of death in the United States and about 1,638,910 new cancer cases were diagnosed in 2012 (American Cancer Society. Cancer Facts & Figures 2012 Atlanta, Ga: American Cancer Society; 2012). Around 2.4 million new cases of cancer were diagnosed in EU countries in 2008 with 55 % occurring among males and 45 % among females (Ferlay J, Shin HR, Bray F, et al. (2010). GLOBOCAN 2008 v1.2, Cancer Incidence and Mortality Worldwide, International Agency for Research on Cancer, Lyon). Cancer has become one of the ten leading causes of death in India; officially recorded over half a million deaths due to cancer in 2011—5.35 lakh as against 5.24 lakh in 2010.

Cyclin-dependent kinase (CDK2) is considered as a potential target for treatment of cancer [1]. 1KE8 is a cyclin-dependent kinase and this docking study was conducted to find the 1KE8 inhibitor. 1KE8 belongs to a family of protein kinases first discovered for their role in regulating the cell cycle. Indoles and chromenes are heterocyclic ring systems displaying a broad spectrum of biological activities. The stereo specific structural descriptors have made this class of compounds privileged drug candidates. They are clinically effective antifungal, antioxidant, hypertensive, antiallergenic and anti-tumor [2–7]. Modification in their structure has offered a high degree of diversity that has proven useful for the development of new therapeutic agents having improved potency and lesser toxicity.

Drug design is the inventive process of finding new drug molecules based on the knowledge of a biological target. Computer-aided drug design uses computational principle as applied to chemistry to discover, enhance, or study drugs and related biologically active molecules. Ligand based drug design depends on the knowledge of the molecules that bind to the biological target, whereas structure based drug design relies on the knowledge of the three dimensional structure of the biological target. The most fundamental goal is to predict whether a given molecule will bind to a target and if so how strongly [8–10].

A. K. V.A (✉)
Department of S & H (Computer Applications), Sathyabama University, Chennai, India
e-mail: akva1234@gmail.com

K. Mohan
SVN College of Engineering, Mavelikkara, Kerala, India

S. Riyaz
Gokaraju Rangaraju Institute of Engineering & Technology, Hyderabad, India

Methods

Protein preparation

The crystal structure (1KE8) used in this study contains CDK2 complexes with the inhibitor LS4. The protein structure was refined using Protein Preparation Wizard implemented in Maestro 9.3 by adding hydrogen atoms, assigning bond orders and capping the N and C termini (Maestro, Version 9.3, Schrödinger, LLC, New York, NY, 2012). The hydrogen bonding network was optimized by predicting histidine tautomeric and ionization states, sampling hydroxyl and thiol hydrogen orientations and flipping terminal amide groups of glutamine and asparagines residues. Finally water molecules were removed and the structure was minimized briefly using Impref tool to relieve steric clashes (Schrödinger Suite 2011 Schrödinger Suite; Epik version 2.2, Schrödinger, LLC, New York, NY, 2011; Impact version 5.7, Schrödinger, LLC, New York, NY, 2011; Prime version 2.3,Schrödinger, LLC, New York, NY, 2011). The minimization was terminated when all atom rmsd reached a maximum of 0.3 Å.

Binding site analysis

The binding site of the protein was computed with SiteMap [11, 12]. SiteMap characterizes a binding site using a grid-based approach where properties are computed at each grid point and rules are used to determine which grid points can be combined to create a binding site. SiteMap calculation begins with an initial search stage that determines one or more regions on or near the protein surface, called *sites*, that may be suitable for binding of a ligand to the receptor. The search uses a grid of points, called *site points*, to locate the sites. In the second stage, contour maps (*site maps*) are generated, producing hydrophobic and hydrophilic maps. The hydrophilic maps are further divided into donor, acceptor, and metal-binding regions.

Docking studies

All the designed molecules were prepared using LigPrep module of Schrödinger by generating expand protonation and tautomeric states at 7.0±2.0 pH units. The compounds were then docked flexibly using Glide XP 5.8, most of these compounds are fragments (molecular weight ~350) we increased the number of poses per ligand for the initial docking stage to 50,000, used a wider scoring window of 500.0 kcal mol^{-1} for keeping initial poses, and kept the best 1000 poses per ligand for energy minimization. This allowed for a much larger number of poses to be scored with the more accurate scoring function in Glide. The "Write XP descriptor information" was chosen during the docking run (an option in the Glide interface), which writes a file containing atom-level energy terms such as hydrogen-bond interactions, electrostatic interaction, hydrophobic enclosure, and pi–pi stacking interactions. We also subjected the top ten poses per compound to post-docking minimization and requested the top ten poses to be returned.

Synthetic route

Synthetic route 1

Synthesis of indole-pyramididne-2,4,6 triones (3a-b) A mixture of **1** (0.735 g, 5 mmol), **2** (0.640 g, 5 mmol), L-proline (catalytic amount) and water (35 ml) was stirred at R.T for 30–45 min. The separated reaction mass was, filtered, washed with ethanol (2×5 ml), dried and recrystallized to get (3a and 3b). Schemes1 and 2

5-(1H-Indol-3-yl-methylene)-pyrimidine-2,4,6-trione (3a) Yield: 0.133gr (92 %) ; M.P(°C): >220 ; IR (KBr): 3420 and 3,455 cm^{-1}(broad, two -NH groups of barb.acid), 3,510 cm^{-1} (–NH of indole) ; ^{1}H- NMR (400 MHz, DMSO-d_6/TMS): δ 7.31–9.51 (m,6H) corresponds to 5H aromatic + 1H vinyl proton),11.05 and 11.13 (S, 1H, -NH of barb.acid), 12.73 (1H,br, -NH of indole). M/Z (M^++1): 256; Anal. Calcd. for ($C_{13}H_9N_3O_3$) requires C,61.21; H, 3.55; N,16.36; found C,62.67; H, 3.93; N,16.89.

5-(1-Methyl-1H-indol-3-ylmethylene)-pyrimidine-2,4,6-trione (3b) Yield: 0.149gr (94 %); M.P(°C): >220 ; IR (KBr): 3420 and 3,455 cm^{-1}(broad, two -NH groups of barb.acid) ; ^{1}H-NMR (400 MHz, DMSO-d_6/TMS): δ 3.60 (s,3H, -NCH_3) 7.28–8.72 (m,6H) corresponds to 5H aromatic + 1H vinyl proton),10.90 and 10.98 (s, 1H, -NH of barb.acid); M/Z (M^++1): 270 ; Anal. Calcd. for ($C_{14}H_{11}N_3O_3$) requires C,62.21; H, 4.55; N,15.36; found C,62.67; H, 4.93; N,15.89.

Scheme 1 Synthetic route 1

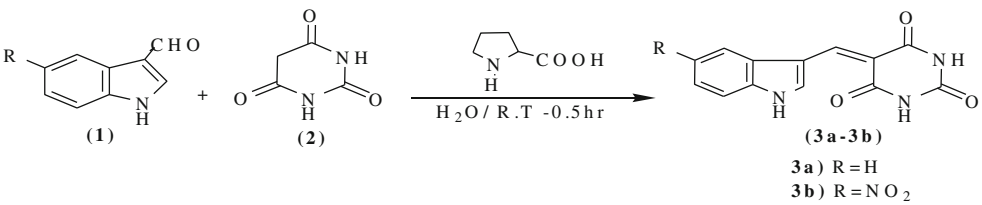

Scheme 2 Synthetic route 2

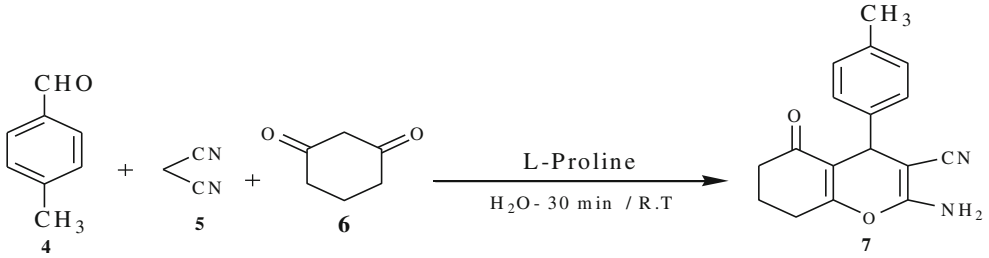

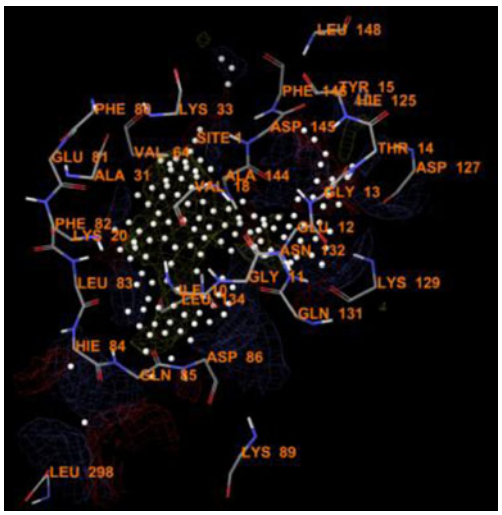

Fig. 1 Binding site analysis of CDK2

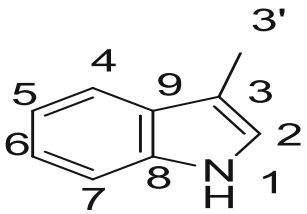

Fig. 2 Structure of indole with numbering

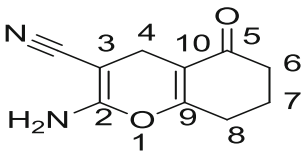

Fig. 3 Structure of chromene with numbering

Synthetic route 2

Synthesis of Chromene −3-carbonitril (7) A mixture of p-methylbenzaldehyde (**4**, 3.0 mmol), malononitrile (**5**, 3.0 mmol), and cyclohexane-1,3-dicarbonyl compound (**6**, 3.0 mmol), L-Proline (catalytic amount) and water (25 ml) was stirred at R.T for 20–30 mins. The solid was collected by filtration, washed with water (2×25 ml), dried in a vacuum oven and recrystallized from EtOH to get **7**.

2-Amino-5-oxo-4-p-tolyl-5,6,7,8-tetrahydro-4H-chromene-3-carbonitrile (7) IR (KBr): 3415, 3325 (unequal doublet, asymmetric & symmetric stretching of -NH_2), 2195 (−CN group, sharp), 1710 (−C=O of chromene moiety, sharp) ; ^{1}H-NMR (400 MHz, DMSO-d6/TMS): δ 1.86–2.62 (m,6H –$(CH_2)_3$), 3.82 (s, 3H, -OCH_3), 4.18 (s,1H,) 6.14 (S, 2H, -NH_2, D_2O exchangeable), 7.15–7.30 (4 H, m, ArH): Anal. Calcd. for ($C_{17}H_{16}N_2O_2$) requires C, 72.84; H, 5.75; N, 9.99; found C, 725.84; H, 5.45; N, 9.59; LC-MS:m/z: (M^++1): 281.

Results and discussion

Indole and chromene moieties were proved to have broad range of activities [2–7]. In-order to find the potential indole and chromene derivatives against CDK2 receptor, a focused library on chromene and indole moieties based on the structural features of ATP binding pocket of CDK2 was constructed. Binding site analysis was performed to analyze the structural features of binding pocket of CDK2 using SiteMap tool of Schrödinger software. The results of the binding site analysis were shown in Fig. 1. The complementary regions generated by the SiteMap against the CDK2 binding site are useful in

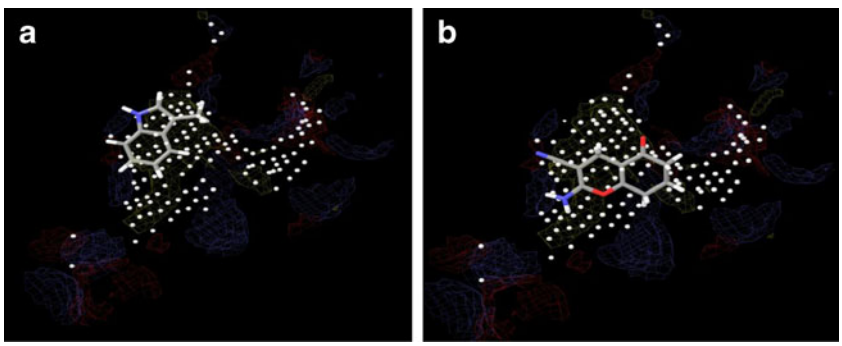

Fig. 4 Superopsitioning of **a** indole and **b** chromene moieties on the SiteMap generated for the binding site of CDK2; yellow, blue and red represents hydrophobic, donor, and acceptor maps respectively

Table 1 Docking scores of indoles

Compound Name	Structures	Glide Score
I_1	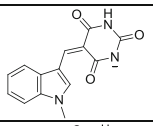	-5.18
I_2	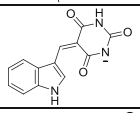	-7.39
I_3	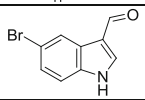	- 7.13
I_4	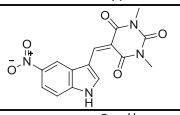	-6.55
I_5	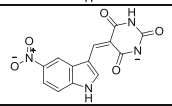	-5.98
I_6	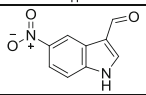	-6.5
I_7	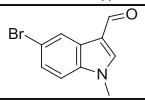	-6.79
I_8	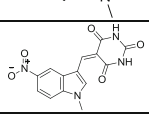	-7.21
I_9	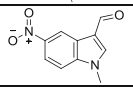	6.26
I_{10}	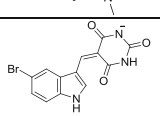	-6.34
I_{11}	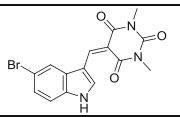	-7.32
I_{12}	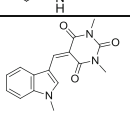	- 5.6
I_{13}	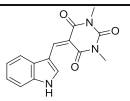	5.62
I_{14}	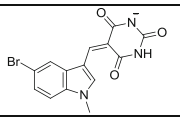	-6.73
I_{15}	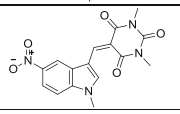	-4.8

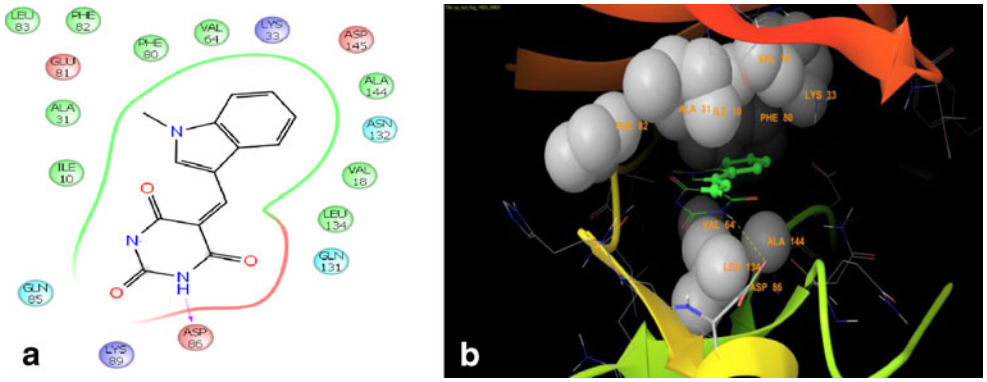

Fig. 5 **a** 2D plot of docking pose of the compound I_1 against CDK2. **b** Docking pose of compound I_1 inside the binding pocket of CDK2 with hydrogen bond and hydrophobic interactions

evaluating in the pocket and thus useful in designing the potential inhibitors. As illustrated in the figure the red, blue and yellow regions are the complementary acceptor, donor and hydrophobic regions respectively. The large hydrophobic region is occupied in the middle and surrounded by the donor and acceptor regions. For designing of novel compounds, the basic moiety can be occupied in the hydrophobic region and its substituents can be dictated by these donor and acceptor regions for activity and selectivity (Figs. 2 and 3).

The indole and chromene fragments were docked into the binding pocket of CDK2 using extra precision mode of Glide. In order to increase the sampling space inside the pocket for these fragments, initial pose filters were increased to 6000 poses per ligand for initial phase of docking and for energy minimization, poses were increased to 1000. The best scoring poses of two moieties selected from the docking results were superimposed onto the sitemap in-order to identify the complementary substituents to be attached on these moieties for lead optimization. Figure 4 (a and b) illustrates the important positions on these moieties for substitutions based on the mapping of docked poses of two moieties on sitemap. The indole moiety was well placed inside the hydrophobic pocket (yellow region), orienting its NH group to the small donor region of site map which complements with the Glu81 of hinge region. The donor region mapping near the 8th position of indole ring which represents the acceptor group (CO) of hinge region amino acid, Leu83 indicates that at this position substituents with donor elements favors activity. At 3rd position of the indole ring small hydrophobic pocket and a little farther from this position a large acceptor region was available. The basic moiety contains methyl group at this position and the bulky substitutes with acceptors on 3rd will favors activity. At 5th position the site map shows hydrophobic region and near to that a large donor region. The groups with hydrophobic with donor substituent favors the activity

The super positioning of best docking pose of chromene moiety on sitemap was shown in the Fig. 4b. As depicted in the Fig. 4b, the major portion of chromene ring was positioned in the hydrophobic region. The amino group substituted at 2nd position was mapped to the donor region (blue region) which complements the back bone CO of Glu 81. The electron rich CN attached at 3rd position of chromene ring projected into the acceptor region (red) which complements the backbone NH of Leu83. These two major interactions correspond to the hinge region of the receptor. At 4th position a large hydrophobic pocket was available for the substitution of bulky groups. A blue and red contour appeared near the 6th position which indicates that the groups with both donors and acceptors favors higher activity. A small hydrophobic pocket followed by large donor region is available at 7th position of the moiety and hence methyl substituted donor groups are favorable at this position. A large blue counter near the 8th position signifies the presence of substituents with donor groups is

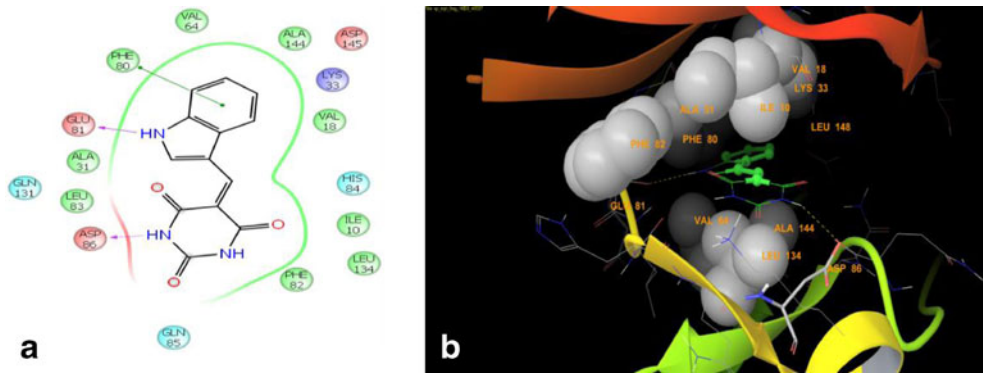

Fig. 6 **a** 2D plot of docking pose of the compound I_2 against CDK2. **b** Docking pose of compound I_2 inside the binding pocket of CDK2 with hydrogen bond and hydrophobic interactions

Table 2 Docking scores of chromenes

Compound Name	Structures	Glide Score
C_1	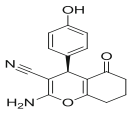	-6.09
C_2	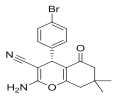	-5.37
C_3	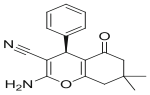	-7.05
C_4	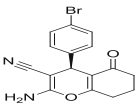	-6.11
C_5	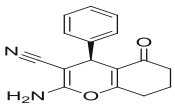	-6.67
C_6	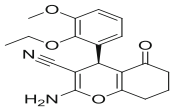	-3.0
C_7	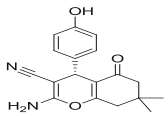	-6.12
C_8	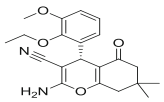	-3.41
C_9	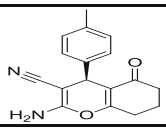	-9.95

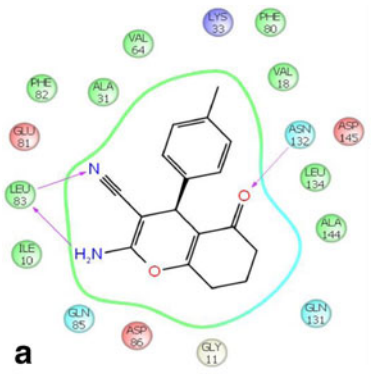

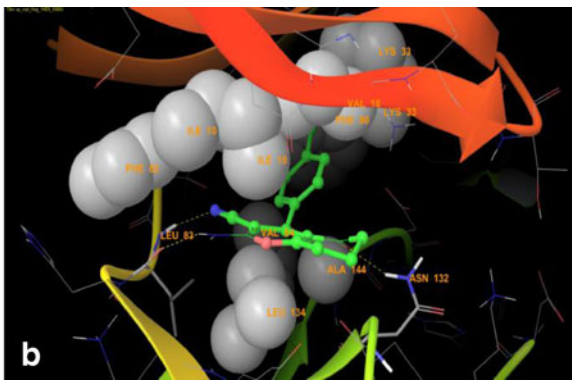

Fig. 7 **a** 2D plot of docking pose of the compound C_9 against CDK2. **b** Docking pose of compound C_9 inside the binding pocket of CDK2 with hydrogen bond and hydrophobic interactions; yellow dotted lines represents the hydrogen bond interactions between ligand receptor; the atoms of C_9 (represented in ball) show hydrophobic interaction amino acids (represented in grey color)

Table 3 MCF-7 cell line values of S1, S2, and S3

	Optical density (OD)					
Concentration	1st	2nd	3rd	Mean OD	Mean OD—blank	% of inhibition
Blank	0.134	0.148	0.118	0.133333333		
Dox	0.458	0.695	0.361	0.504666667	0.371333333	30.63511831
No treatment	0.759	0.692	0.555	0.668666667	0.535333333	
S1 2 mg/ml	0.854	0.771	0.734	0.786333333	0.653	−21.98007472
S1 1 mg/ml	0.842	0.729	0.776	0.782333333	0.649	−21.23287671
S1 0.5 mg/ml	0.628	0.638	0.665	0.643666667	0.510333333	4.669987547
S1 0.25 mg/ml	0.792	0.718	0.8	0.77	0.636666667	−18.92901619
S1 0.1 mg/ml	0.727	0.781	0.663	0.723666667	0.590333333	−10.2739726
S1 0.05 mg/ml	0.692	0.885	0.813	0.796666667	0.663333333	−23.91033624
S3 2 mg/ml	0.213	0.191	0.32	0.241333333	0.108	79.8256538
S3 1 mg/ml	0.42	0.473	0.452	0.448333333	0.315	41.15815691
S3 0.5 mg/ml	0.752	0.68	0.795	0.742333333	0.609	−13.76089664
S3 0.25 mg/ml	0.793	0.909	0.663	0.788333333	0.655	−22.35367372
S3 0.1 mg/ml	0.893	0.686	0.752	0.777	0.643666667	−20.2366127
S3 0.05 mg/ml	0.6	0.674	0.614	0.629333333	0.496	7.347447073
Blank	0.007	0.01	0.011	0.009333333		
No treatment	0.52	0.65	0.623	0.597666667	0.588333333	
S2 2 mg/ml	0.268	0.286	0.258	0.270666667	0.261333333	55.58073654
S2 1 mg/ml	0.251	0.263	0.253	0.255666667	0.246333333	58.13031161
S2 0.5 mg/ml	0.299	0.32	0.319	0.312666667	0.303333333	48.44192635
S2 0.25 mg/ml	0.384	0.357	0.345	0.362	0.352666667	40.05665722
S2 0.1 mg/ml	0.409	0.43	0.411	0.416666667	0.407333333	30.76487252
S2 0.05 g/ml	0.423	0.444	0.449	0.438666667	0.429333333	27.02549575

favored at this position. In the present work we have focused mainly on the 4th position for adding the substituents and designed nine compounds by adding substituted phenyl groups at this position (Table 2).

In order to identify the better analogues from the indole derivatives, all the analogues were docked into the receptor against CDK2 using Glide extra precision. The result of the docking study is illustrated in Table 1. Among the indoles (Figs. 5 and 6), I_2 showed a good glide score of −7.39 kcal mol^{-1}. The compound showed strong hydrogen bond and hydrophobic interactions with the receptor NH group of indole moiety showed hydrogen bond with Glu81 of hinge region due to the presence of large red region near the 3rd position of the indole ring. The substituent pyrimidine-2,4,6-trione has been well placed in this region and exhibited strong hydrogen bond with side chain COO group of Asp 86 (Fig. 6b). The indole moiety has been well enclosed in the hydrophobic region of the sitemap (Fig.6b) showing strong hydrophobic interactions with the amino acids Phe82, Ile10, Phe80, Val18, Lys33, Val64, Alo32, Leu134 and Ala144. Due to the presence of strong hydrophobic and hydrogen bond interactions, the compound showed a high affinity with receptor. Hence we selected this compound from the indole derivatives for synthesis and biological testing. In order to test the importance of hinge region interactions, that is with Glu86, we also selected the indole (I_1) which contains substituent CH3 at N1 position for biological testing. Due to the presence of methyl substitution, it loses its hydrogen bond with Glu86 (Fig. 5b).

With a view to identify the best interacting compounds among the designed indole and chromene analogues, docking studies were carried out against CDK2 receptor using Glide extra precision. All the analogues were docked into the binding pocket of CDK2 receptor and the results are tabulated in Tables 1 and 2. As illustrated in the tables, these compounds have glide score in the range between −9.95. 25 kcal mol^{-1} to −3 kcal mol^{-1}. Due to the presence of NH2 and CN group at 2nd and 3rd positions respectively on chromene ring, it showed hydrogen bond interaction with hinge region amino acid, Leu83. Among the chromenes analyzed, the compound C_9 showed a maximum glide score of −9.95 kcal mol^{-1}. Along with hydrogen bond interactions with Leu83, this compound exhibited hydrogen bond with side chain NH2 group of ASN132 with its CO group. Due to the substitution of para-methyl phenyl at 4th position, it is well enclosed in the hydrophobic region of the sitemap (Fig. 7b) and showed strong hydrophobic interactions with the amino acids Phe82, Ile10, Phe80, Val18, Lys33, and Val64. These hydrophobic interactions and hydrogen bond interactions cumulatively made the compound to bind with

Table 4 HeLa cell line values of S1, S2, and S3

	Optical density (OD)					
Concentration	1st	2nd	3rd	Mean OD	Mean OD—blank	% of inhibition
Blank	0.126	0.082	0.105	0.104333333		
Dox	1.371	1.357	1.473	1.400333333	1.296	37.36104398
No treatment	2.137	2.105	2.278	2.173333333	2.069	
S1 2 mg/ml	1.052	1.052	1.093	1.065666667	0.961333333	53.53632995
S1 1 mg/ml	1.303	1.226	1.165	1.1955	1.091166667	47.26115676
S1 0.5 mg/ml	1.35	1.081	1.189	1.206666667	1.102333333	46.72144353
S1 0.25 mg/ml	1.16	1.072	1.205	1.205	1.100666667	46.80199774
S1 0.1 mg/ml	1.306	1.206	1.128	1.213333333	1.109	46.39922668
S1 0.05 mg/ml	1.079	1.272	1.537	1.296	1.191666667	42.40373772
S3 2 mg/ml	0.738	0.648	0.698	0.694666667	0.590333333	71.46769776
S3 1 mg/ml	0.911	0.745	0.958	0.8515	0.747166667	63.88754632
S3 0.5 mg/ml	1.293	1.09	0.932	1.105	1.000666667	51.63525052
S3 0.25 mg/ml	0.966	1.284	1.247	1.125	1.020666667	50.66859997
S3 0.1 mg/ml	1.336	1.338	1.36	1.344666667	1.240333333	40.0515547
S3 0.05 mg/ml	1.554	1.56	1.634	1.582666667	1.478333333	28.54841308
Blank	0.007	0.01	0.011	0.009333333		
S2 2 mg/ml	0.869	0.925	0.903	0.899	0.889666667	21.17542823
S2 1 mg/ml	0.918	0.903	0.955	0.925333333	0.916	18.84229179
S2 0.5 mg/ml	0.866	0.997	1.026	0.963	0.953666667	15.50502067
S2 0.25 mg/ml	0.984	0.919	1.01	0.971	0.961666667	14.79621973
S2 0.1 mg/ml	0.821	0.822	0.89	0.844333333	0.835	26.01890136
S2 0.05 mg/ml	0.847	0.99	0.894	0.910333333	0.901	20.17129356

the receptor with high affinity. Hence C_9 was selected from the chromene analogues for synthesis and wet lab biological testing.

Biological testing (MTT ASSAY)

MCF-7 cell line

Procedure

5×10^3 cells of MCF-7 were seeded in a well with 100 μl media per well in a 96 well plate. This was incubated overnight at 37 °C/5 % CO_2. Three wells were left blank. Next the stock test sample was prepared at the concentration of 4 mg/ml. And this was serially diluted to 2 mg/ml, 1 mg/ml, 0.5 mg/ml, 0.2 mg/ml, and 0.1 mg/ml in the medium. These diluted samples were added in triplicate to the cells, with each well getting 100 μl of the test sample. The negative and positive controls were 100 μl of medium and 1 μg/ ml Doxorubicin respectively. This was mixed and incubated at 37 °C/5 % CO_2 for 48 h. After 48 h 20 μl of 5 mg/ml MTT in PBS was added to each well and incubate at 37 °C/5 % CO_2 for 4 h. The medium was aspirated and 200 μl of dimethyl sulfoxide (DMSO) was added to each wells. Optical density of these mixtures were measured using microplate reader at 570 nm and the percentage inhibition was calculated as follows:

$$\%\ \text{Inhibition} = 100-\left[\left(\text{Mean OD for test sample}\Big/\text{mean OD for the control}\right)\times 100\right]$$

Negative values were considered as no inhibition or lysis and the concentration at which the sample exhibits 50 % of its maximum activity (ED50) was calculated using the ED50 plus v1.0 software (Table 3).

Inference

No cytotoxicity effect observed by sample S1 on MCF-7 Cells

ED_{50} of sample S3 on MCF-7 Cells is 1.228 mg/ml
ED_{50} of sample S2 on MCF-7 Cells is 0.58 mg/ml

HeLa cell line

The same procedure of MCF-7 cell line was repeated in HeLa cell line (Table 4).

Inference

ED_{50} of S1 on HeLa Cells is 1.5 mg/ml
No cytotoxicity effect observed by sample S2 on HeLa Cells
ED_{50} of S3 on HeLa Cells is 240.71 μg/ml (0.240 mg/ml).

The above biological study reveals that the samples S2 and S3 show anti cancer activity.

Conclusions

The indole and chromene derivatives active against CDK2 receptor were designed based on the structural features of ATP binding pocket of CDK2. Binding site analysis was performed to analyze the structural features of binding pocket of CDK2 and generated red, blue and yellow regions are the complementary acceptor, donor and hydrophobic regions respectively. The large hydrophobic region was occupied in the middle and surrounded by the donor and acceptor regions. Based on these structural features of binding pocket, chromene and indole derivatives were designed and docked to evaluate the binding affinity. Among the chromene derivatives, the compound (C_9) with para-methyl phenyl _substitution at 4th position showed a maximum glide score of −9.95 kcal mol^{-1}. In the case of indole derivatives the compound (I_2) with the substituent pyrimidine-2,4,6-trione at 3rd position of the indole moiety, showed a good glide score of −7.39 kcal mol^{-1}. Both the compounds showed high affinity due to their strong hydrophobic interactions and hydrogen bond interactions with receptor. These compounds were synthesized and tested biologically, and they showed activity against MCF-7 and HELA cell lines in MTT assay.

References

1. Malumbres M, Barbacid M (2009) Cell cycle, CDKs and cancer: a changing paradigm. Nat Rev Cancer 9:153–166
2. Chinni SR, Li Y, Upadhyay S, Koppolu PK, Sarkar FH (2001) Indole-3-carbinol (I3C) induced cell growth inhibition, G1 cell cycle arrest and apoptosis in prostate cancer cells. Oncogene 20:2927–2936
3. Naik R, Nixon S, Lopes A et al (2006) A randomized phase II trials of indole-3-carbinol in the treatment of vulvar intraepithelial neoplasia. Int J Gynecol Cancer 16(2):786–790
4. Bell MC et al (2000) Placebo-controlled trial of indole-3-carbinol in the treatment of CIN. Gynecol Oncol 78(2):123–129
5. Rampa A, Bisi A, Belluti F, Gobbi S, Piazzi L, Valenti P, Zampiron A, Caputo A, Varani K, Borea PA, Carrara M (2005) Homopterocarpanes as bridged triarylethylene analogues: synthesis and antagonistic effects in human MCF-7 breast cancer cells. Farmaco 60(2):135–147. doi:10.1016/j.farmac.2004.09.006
6. Quan-Bin H, Nian-Yun Y, Hong-Lei T, Chun-Feng Q, Jing-Zheng S, Chang DC, Shi-Lin C, Luo KQ, Hong-Xi X (2008) Phytochemistry 69:2187
7. Coudert P, Coyquelet JM, Bastide J, Marion Y, Fialip J (1988) Ann Pharm Fr 46:91
8. Blundell TL (1996) Structure-based drug design. Nature 384(6604 suppl):23–26
9. Whittle PJ, Blundell TL (1994) Protein structure-based drug design. Annu Rev Biophys Biomol Struct 23:349
10. Kuntz ID (1992) Structure-based strategies for drug design and discovery. Science 257:1078
11. Halgren T (2009) Identifying and characterizing binding sites and assessing drug ability. J Chem Inf Model 49:377–389
12. Halgren T (2007) New method for fast and accurate binding-site identification and analysis. Chem Biol Drug Des 69:146–148